Surface phase transitions of Pt(110) studied by desorption dynamics of product CO_2 in steady-state CO oxidation

I. Rzeznicka
Graduate School of Environmental Earth Science, Hokkaido University, Sapporo 060-0810, Japan

L. Morales de la Garza
Centro de Ciencias de la Materia Condensada, Universidad Nacional Autonoma de Mexico, Ensenada, BC, Mexico

T. Matsushima[a)]
Catalysis Research Center, Hokkaido University, Sapporo 060-0811, Japan

(Received 29 October 2001; accepted 3 May 2002)

The transformation of (1×2) into (1×1) on a Pt(110) surface in the course of CO oxidation was studied through the analysis of both angular and velocity distributions of desorbing product CO_2 and low-energy electron diffraction (LEED) intensity. The intensity of half-order LEED spots decreased quickly, showing the beginning of the transformation of $(1\times2)\rightarrow(1\times1)$ just below the kinetic transition, where the rate-determining step switched from CO adsorption to O_2 dissociation. On the other hand, the angular distribution of desorbing CO_2 sharply changed at a CO pressure far above the kinetic transition, where (1×2) domains disappeared. Below this approximate CO pressure, CO_2 was mostly formed on (1×2) domains regardless of its reduced area. © *2002 American Vacuum Society.* [DOI: 10.1116/1.1488945]

I. INTRODUCTION

In steady-state CO oxidation on platinum metals, there is a critical CO pressure at which the rate-determining step switches from CO adsorption to O_2 dissociation. Around this kinetic transition, the surface species change from O(a) $>$CO(a) to O(a)$<$CO(a).[1] On Pt(110) above the critical pressure, the surface structure changes from (1×2) to (1×1) when the CO pressure is high enough to reach the threshold CO(a) coverage for the transformation.[2] Around the kinetic transition, the angular distribution of desorbing CO_2 also changes from a two-directional form collimated along the local normal of declining (111) terraces of the (1×2) structure to normally directed desorption.[3] This is because desorbing product CO_2 carries a high excess in the translational energy and holds the site orientation for CO_2 formation.[4] Thus, the angle-resolved (AR) product desorption measurements provide surface–structural information.

This article is the first to report measurements of angular and velocity distributions of desorbing CO_2 and low-energy electron diffraction (LEED) spot intensity at steady-state conditions. The kinetic transition can be determined from a sharp decrease of either the CO_2 signal or the intensities of the half-order LEED spots. On the other hand, a complete surface–structural transformation can be confirmed only by a sharp change in the angular distribution of CO_2.

The chemical oscillation on Pt(110) takes place at somewhat higher CO pressures than the kinetic transition and is explained by the surface–structural change between (1×1) and (1×2) forms.[5] In the course of the catalyzed reaction near the oscillation condition, CO(a) and O(a) form separate domains with peculiar patterns,[6,7] and those domains move on the surface. CO(a) domains are on the (1×1) form, and O(a) domains are on the (1×2) form.[6] This situation suggests that CO_2 is merely formed on (1×2) domains and not on the boundary between both domains[8] because of the much higher mobility of CO(a) over O(a).[9] Furthermore, CO(a) has a long surface-residence time on an oxygen-covered area at elevated temperatures until its removal as CO_2.[10]

AR measurements of desorbing CO_2 were applied under steady-state conditions far from the chemical oscillation, especially between the kinetic transition and the site- switching point, where separate domains of CO(a) and O(a) were stable. CO_2 was mostly emitted from (1×2) domains into inclined ways in a plane along the [001] direction until the (1×2) domains mostly disappeared. This observation indicates a high capacity of (1×2) domains to produce CO_2.

II. EXPERIMENTS

The apparatus consists of a reaction chamber, a chopper house, and an analyzer.[11] All chambers are evacuated by individual pumping systems. The reaction chamber has reverse-view LEED and x-ray photoelectron spectroscopy optics, an Ar^+ gun, and a quadrupole mass spectrometer (QMS). In the chopper house, a correlation chopper yielded a time resolution of 20 μs at 98.04 Hz rotation.[12] The arrival times at the ionizer of another QMS in the analyzer were registered on a multichannel scalar running synchronously with the chopper rotation. A Pt(110) single crystal of 10 mm diameter and 1 mm thickness was mounted on the top of a rotatable manipulator.

During AR steady-state measurements, the chopper disk was stopped at the position where an open slot was in front of the first slit. The partial pressures of ^{13}CO (P_{CO}) and O_2 (P_{O_2}) were kept constant by dosing gases continuously. The

a)Author to whom all correspondence should be addressed; electronic mail: tatmatsu@cat.hokudai.ac.jp

crystal was rotated to change the desorption angle (θ; polar angle) in the normally directed plane, including the [001] direction.[13] Hereafter; ^{13}C is simply designated as C. The partial pressures of CO and O_2 were monitored with a differentially pumped QMS to shield the filament light from the LEED optics.

III. RESULTS

A. Reaction rate and angular distribution

The steady-state CO_2 formation was monitored in the AR form. It was determined by QMS in the analyzer as the difference (ΔCO_2) between the signal at the desired angle and that when the crystal was away from the line-of-sight position. The CO_2 signal at $\theta=25°$ and 0° increased linearly with increasing P_{CO} below the kinetic transition, where it decreased and showed negative orders in CO, as shown in Fig. 1(a). The region below the kinetic transition is called the ''active region,'' and that above it is the ''inhibited region.''

The angular distributions of desorbing CO_2 in the plane along the [001] direction are shown in Figs. 1(b)–1(e). At around the kinetic transition, the distribution split into two inclined components collimated at $\theta\pm25°$ [Fig. 1(b)]. Far above the transition point, the angular distribution became sharp along the surface normal [Fig. 1(e)]. It should be noted that the distribution was well split above the kinetic transition [Fig. 1(c)].

Figure 1(a) shows the AR signals at both $\theta=25°$ and $\theta=0°$ as a function of P_{CO}. In the active region, the signal at $\theta=25°$ run above that at $\theta=0°$, confirming the aforementioned two-directional desorption. In the inhibited region, the signal preference at $\theta=25°$ continued to a certain CO pressure, and then the signal at $\theta=0°$ overcame that at 25°. The CO pressure at which the CO_2 signal at $\theta=25°$ becomes equal to that at $\theta=0°$ is called ''site switching'' because of the sharp angular distribution change.[3] The CO pressure required for the site switching was about four times higher than that at the kinetic transition. Above the site-switching, the signal in the normal direction was more intense than that at $\theta=25°$. Above $P_{O_2}=3\times10^{-5}$ Torr and below $T_S=500$ K, no separation was found between the kinetic transition and the site switching, and the distribution became a normally directed form just above the kinetic transition, as shown in Sec. III D.

B. Velocity distribution

The translational energy can be used to examine the presence of a desorption component because it is maximized at the collimation angle in the repulsive desorption.[4,14]

The translational energy of CO_2 was maximized at around $\theta=25°$ in the active region, being consistent with the two-directional desorption. Typical velocity distributions at $T_S=490$ K are shown in Fig. 2. The curve always showed a single desorption component, i.e., at the present low CO pressure, the slow component described by a Maxwellian distribution at the surface temperature was negligibly small. Each distribution curve was fitted to a single modified Max-

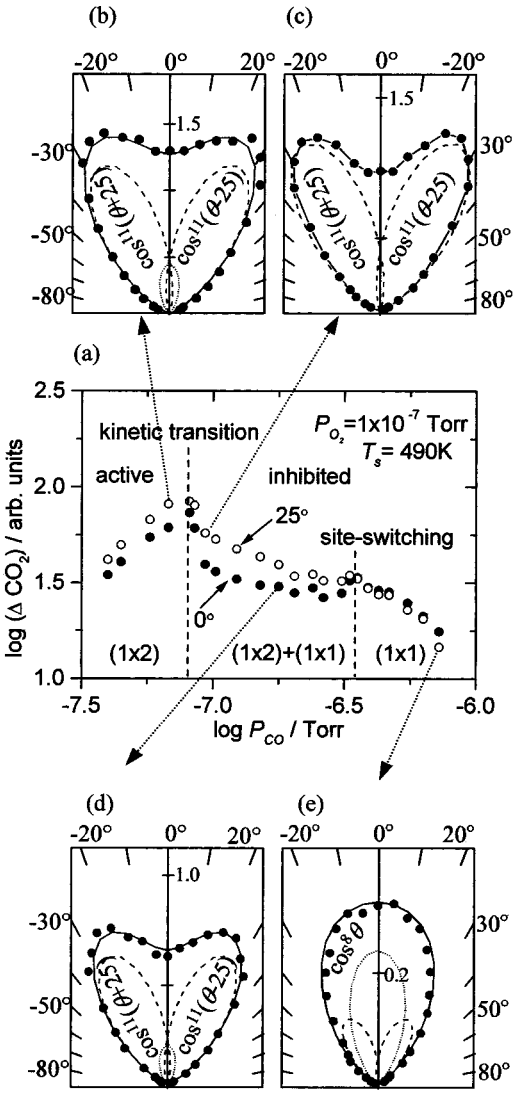

FIG. 1. (a) Steady-state AR CO_2 signals observed at $\theta=25°$ and $\theta=0°$ with CO pressures at $P_{O_2}=1\times10^{-7}$ Torr and $T_S=490$ K. [(b)–(e)] Angular distributions of CO_2 in the plane along the [001] direction are shown in polar coordinates. The signal on the ordinate was normalized to that in the normal direction at the insert (c). Typical deconvolutions are drawn by broken and dotted curves.

wellian form. The resultant energy is shown in the temperature units as $T_{\langle E\rangle}=\langle E\rangle/2k$, where $\langle E\rangle$ is the mean translational energy and k is the Boltzmann constant. In the active region, the value reached 1850±100 K at $\theta=25°$ and 1600±40 K at the normal direction. This maximized translational temperature at $\theta=25°$ and observed two-directional desorption indicate CO_2 formation on the declining terraces of (1×2) domains. This situation held even above the kinetic transition below the site switching since the translational temperature at $\theta=25°$ was still higher than the value at $\theta=0°$. Above the site switching, the value at $\theta=25°$ decreased to 1550±40 K, and the value at $\theta=0°$ increased up to 1720±100 K, indicating that the normally directed desorption started to be dominant. This observation is consistent with an enhanced normally directed desorption component above the site switching, as discussed in Sec. IV A.

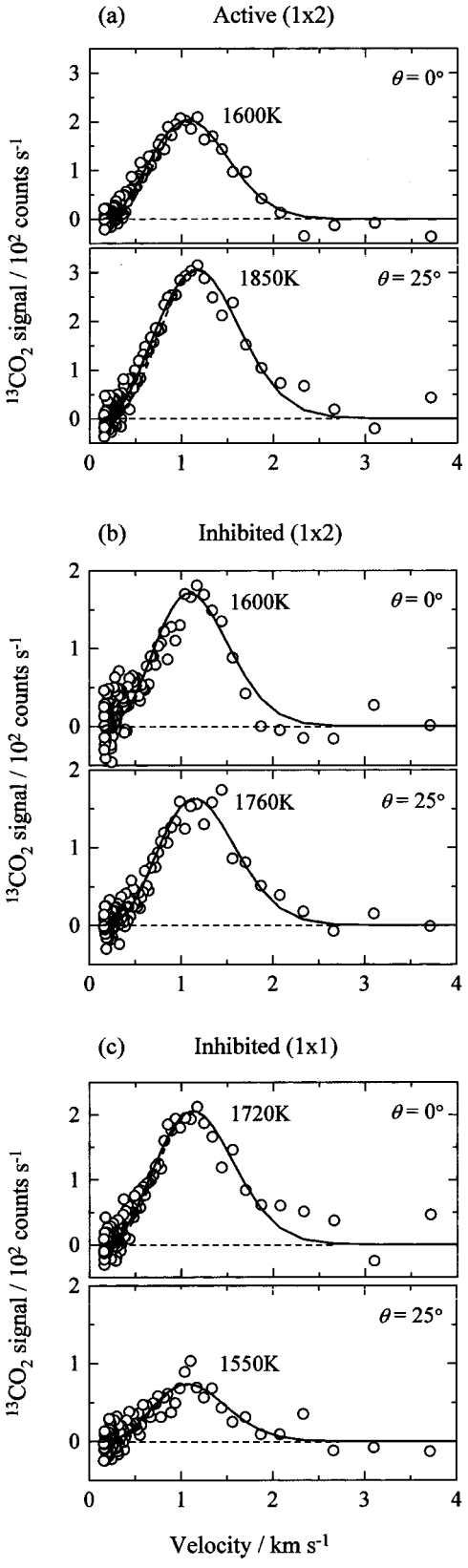

FIG. 2. Velocity distributions of desorbing CO_2 at $\theta=0°$ and $\theta=25°$ at $P_{O_2}=1\times10^{-7}$ Torr and $T_s=490$ K in (a) the active region with $P_{CO}=7.5\times10^{-8}$ Torr, (b) the boundary between the kinetic transition and the site-switching with $P_{CO}=1.6\times10^{-7}$ Torr, and (c) the inhibited region above the site switching at $P_{CO}=5.6\times10^{-7}$ Torr. The solid curves are drawn by a modified Maxwellian distribution. The translational temperatures are inserted.

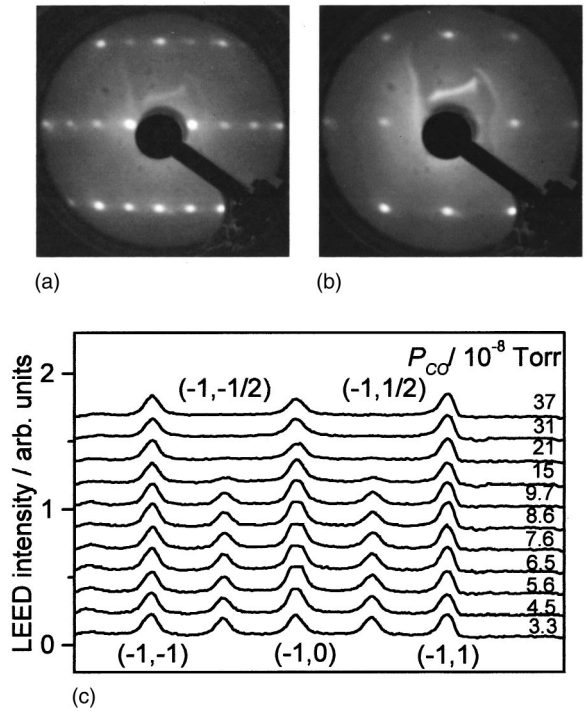

FIG. 3. LEED patterns at 78 eV (a) in the active region and (b) above the site switching. (c) LEED intensity profiles along the [001] direction at various P_{CO} values at fixed P_{O_2} of 1×10^{-7} Torr and $T_S=490$ K.

C. LEED study

A (1×2) LEED pattern was observed in the active region [Fig. 3(a)]. On the other hand, a (1×1) pattern was found near or above the site-switching point, and the half-order spots disappeared [Fig. 3(b)]. The intensity profile along the [001] direction was monitored by a charge coupled device Video system at the acceleration voltage of 78 eV. The LEED patterns were taken over a long integration of 5 s because of the reduced beam current to the level of nonvisible spots. Such measurements were performed after the steady-state reaction condition had been established. The intensities of the half-order spots were significant at low pressures of CO and disappeared at higher CO pressure [Fig. 3(c)]. The intensity of one of the half-order spots, which is due to the (1×2) domains, is plotted against P_{CO} in Fig. 4. With increasing P_{CO}, it decreased quickly in the active region close to the kinetic transition. It reached about a half value at the kinetic transition point and decreased further to the constant background level before the site switching. On the other hand, the integral order spot intensity slightly increased in the active region with increasing P_{CO} and decreased slightly above the kinetic transition. It should be noted that the (1×2) domains quickly became weak while the two-directional CO_2 desorption was still major.

The half-order LEED spot intensity is merely due to (1×2) domains. Its spot width did not change throughout the aforementioned measurements, suggesting that the (1×2) domain was larger than the coherent length of LEED optics.[15] We estimated the fraction of the (1×2) domain by assuming that its area was proportional to the half-order spot intensity.

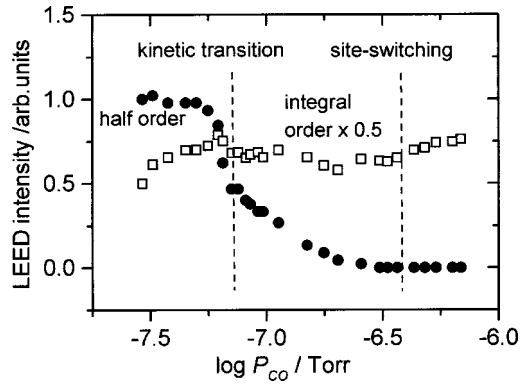

FIG. 4. LEED spot intensity of both half and integral orders vs P_{CO}. The accelerating voltage was 78 eV. Each point was accumulated over 5 s. $P_{O_2}=1\times10^{-7}$ Torr and $T_S=490$ K.

The intensity was normalized to the maximum value in the active region after subtraction of the background level.

D. Borders of the boundary

The kinetic transition shifted to higher P_{CO} values with increasing either T_S or P_{O_2}. The logarithm of the P_{CO} values at the transition is plotted against the reciprocal of the surface temperature in Fig. 5. The line shifted upward with increasing P_{O_2}. It was not sensitive to the surface temperature and the activation energy was estimated to be 5–10 kcal/mol as shown in Fig. 5. On the other hand, the CO pressure at the site-switching seemed to show some limitation at low P_{O_2} as drawn by the dotted line in Fig. 5. The line at 1×10^{-7} Torr of O_2 yielded the activation energy of 31 kcal/mol. The site switching coalesced to the line of the kinetic transition when both lines crossed, i.e., the site switching did not run below the kinetic transition line. Hence, the boundary region between the kinetic transition and the site switching became wider at lower P_{O_2} and higher T_S. At high P_{O_2}, both transitions took place simultaneously and no boundary region appeared. As discussed in Sec. IV C, both lines show the border of surface structure changes, i.e., this figure represents a surface phase diagram.

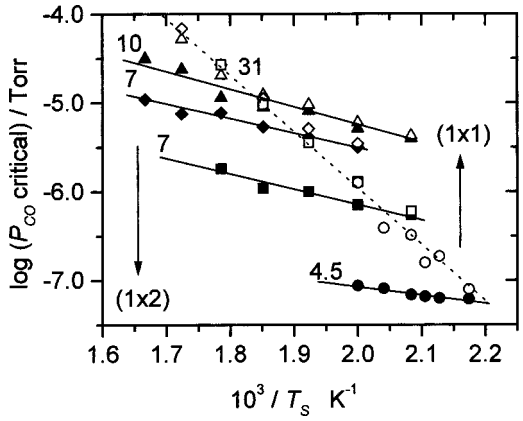

FIG. 5. Surface phase diagram. Logarithms of P_{CO} at the kinetic transition (closed symbols) and site switching (open symbols) are plotted against the reciprocal of T_S at different P_{O_2} values. $P_{O_2}/10^{-6}$ Torr was 0.10 (●,○), 3.0 (■,□), 30 (♦,◇), and 100 (▲,△). The activation energy estimated from the slope is inserted in the unit of kcal/mol. The site-switching line coalesced with the kinetic transition line after crossing. The former did not run below the limit shown by the dotted line. As shown by the arrows, (1×2) domains increased downward, whereas (1×1) domains were enhanced upward.

IV. DISCUSSION

A. Inclined and normally directed desorption

The two-directional desorption reported previously was well reproduced.[3] Under the present low P_{CO} conditions, the normally directed desorption did not become predominant, even at lower P_{CO} in the active region. The reactive CO_2 desorption takes place mostly on declining (111) terraces of the (1×2) form. This is also consistent with the higher translational energy at $\theta=25°$, as shown in Fig. 2(a).[14] The parameters characterizing the two-directional desorption were determined by fitting a power function of the cosine of the desorption angle with the observed data just above the kinetic transition as $\cos^{11}(\theta+25)+\cos^{11}(\theta-25)$ [Fig. 1(c)]. Hereafter, these parameters were used to deconvolute the angular distribution curves.

At high CO pressures above the site switching, CO_2 desorption collimated along the surface normal. The (1×2) reconstruction was lifted into (1×1), since no (1×2) LEED pattern was found. Probably, the CO coverage exceeds the half monolayer enough to reach complete conversion.[5] On the (1×1) form, CO_2 desorption may collimate along the surface normal as observed on Pd(110) and Ir(110).[16,17] The observed high translational energy in the normal direction suggests a sharp angular distribution. However, the apparent distribution was rather broad, as a $\cos^3\theta$ form. This suggests that the normally directed distribution includes a contribution from the inclined component.

The observed angular distribution involved the contribution from more or less both components. Typical deconvolutions of the angular distributions are shown by broken and dotted curves in the upper and lower panel in Fig. 1. The two-directional component was first fitted to the data points, and the remaining signal after its subtraction was fitted into a single power function of $\cos\theta$. The resultant component collimated along the surface normal as $\cos^8\theta$ throughout the conditions used. This sharpness is reasonable when both the high translational temperature of the inclined component and the sharpness of the angular distribution are considered. The apparent distribution of $\cos^3\theta$ above the site switching is too broad to explain the observed high energy.[14]

B. CO_2 formation on (1×2) domains

The contribution to CO_2 formation from the inclined component and the normally directed one was estimated from the AR signal at $\theta=25°$ and $\theta=0°$. Here, the former was fixed to $\cos^{11}(\theta+25)+\cos^{11}(\theta-25)$, and the latter to $\cos^8\theta$. The correction was made by considering the sharpness of each desorption component.[18] The results are shown in Fig. 6(a). In the active region, the inclined component from (1×2) domains increases with increasing P_{CO}. The normally directed

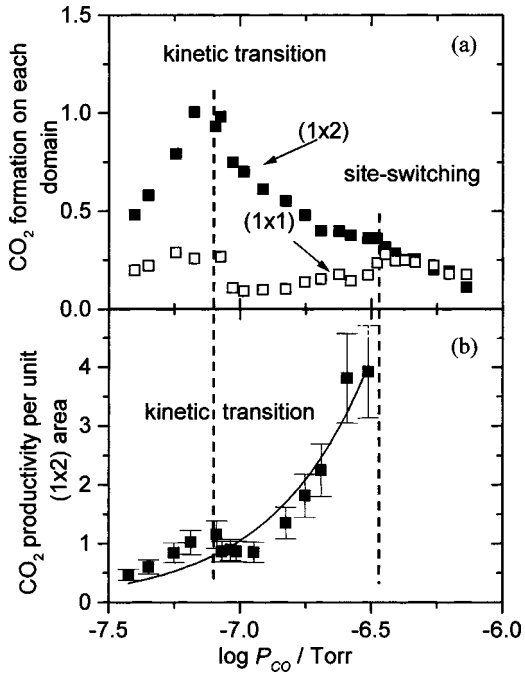

FIG. 6. (a) Variation of the amount of CO_2 in the inclined desorption (■) and the normally directed one (□), with P_{CO} at the steady-state reaction conditions. T_S was 490 K, and P_{O_2} was 1×10^{-7} Torr. (b) The CO_2 productivity on (1×2) domains is the ratio of the total inclined desorption to the half-order LEED spot intensity.

component is noticeable in this region, probably because of the CO_2 formation on the bottom of the (1×2) valley.[3] Above the kinetic transition, the inclined desorption decreased with increasing P_{CO} and reached about 30% of the maximum at the site switching. It should be noted that this CO_2 formation is still significant near the site switching, where the half-order LEED spot already disappeared. The normally directed component becomes noticeable near the site switching. Above the site switching, this component is major, but the inclined component is still noticeable. This comes from the deconvolution procedures involving the normally directed component of $\cos^8\theta$. The aforementioned procedure yields the upper limit of the inclined component. This component decreases somewhat where the normally directed component is assumed as a broader form.

The total CO_2 formation decreased above the kinetic transition, and the inclined component also decreased. The former is limited by O_2 dissociation, and its decrease indicates that the surface is starting to be covered by CO(a). In fact, the formation of CO(a) domains already started below the kinetic transition, as confirmed by the rapid decrease of the half-order LEED spot. Domains of adsorbed CO began to convert (1×2) to (1×1). Nevertheless, the inclined component shared most of the CO_2 formation, indicating that CO_2 is merely formed on (1×2) domains.

This does not exclude the CO_2 formation on (1×1) domains because the normally directed component appeared below the site switching and became major above it, where no (1×2) domains were detected by LEED. The (1×2) domain has a high capacity for CO_2 production, but its capability is limited by the supply of O(a). In other words, the reactivity of O(a) on (1×1) domains is less than that on (1×2). This is reminiscent of the results on Pt(113)(1×2),[18] in which O(a) had a higher reactivity on (111) facets than that on (100) facets. These results are consistent with the smallest adsorption energy of O(a) on (111) among (111), (100), and (110) planes.

The (1×2) domain produces most of the CO_2 even when its share largely decreases. The CO_2 formation rate per unit area must then be increased. The amount of CO_2 formed on (1×2) was divided by the half-order spot intensity. The resultant value increased sharply (as much as ten times) with increasing P_{CO}, as shown in Fig. 6(b). This high productivity can be observed only in AR measurements. The completion of the structure transformation to (1×1) can be examined more sensitively by AR measurements than by LEED because of the high CO_2 productivity on (1×2) domains.

C. Surface phase diagram

At the kinetic transition, CO adsorption balances with the removal of CO(a). The latter proceeds mostly as CO_2. The former is less sensitive to the surface temperature, i.e., no activation energy is required. On the other hand, the latter process has the activation energy of about 24 kcal/mol.[10] However, only 5–10 kcal/mol was obtained from the temperature dependence of P_{CO} at the kinetic transition. This suggests that the reactant density at the transition, especially the CO(a) density, increased with decreasing T_S.

The site switching can be determined only from the angular distribution measurements. The sensitivity is due to the high capacity of CO_2 formation on (1×2) domains. The site switching is completed in a narrow CO pressure range after the disappearance of the (1×2) domain. This critical CO pressure must be the threshold value to reach a half monolayer because of the complete conversion to (1×1).[5] This pressure must shift to higher values with increasing O_2 pressure because of the enhanced removal of CO(a) as CO_2. The observed activation energy was 31 kcal/mol at $P_{O_2}=1\times10^{-7}$ Torr. It is expected to increase more at lower P_{O_2} to the heat of CO adsorption, about 35 kcal/mol.[19] On the other hand, with increasing P_{O_2}, it decreased to 7 kcal/mol at $P_{O_2}=3\times10^{-5}$ Torr, becoming close to the value determined from the oscillation.[2] The physical meaning of the site-switching point became clearer than it was in our previous work, in which a rapid change of surface structures was assumed.[3] In fact, at this point, the structure change from (1×2) to (1×1) form is complete, as confirmed by LEED observation in the present work.

Sustained oscillations can be observed when the kinetic transition overlaps with the site switching because both the transition and switching are required in one oscillation cycle. In fact, between the kinetic transition and the site switching, the oscillation in CO_2 formation disappeared after several cycles even when it happened. The aforementioned boundary will provide a suitable stage for examining product desorption dynamics on reaction sites with different structures.

V. CONCLUSIONS

Angular distributions of desorbing CO_2 and the surface structure transformation of (1×2) into (1×1) on Pt(110) in the course of CO oxidation were studied through the analysis of both AR product measurements and LEED intensity. The results are summarized next.

(1) CO_2 is highly formed on the declining (111) terraces of (1×2) domains, except for high CO pressures above the site switching;
(2) The productivity of CO_2 per unit area of (1×2) domains increases more than ten times in the inhibited region; and
(3) The site switching observed from angular distribution changes is sensitive to the disappearance of (1×2) domains.

ACKNOWLEDGMENTS

One of the authors (I. R.) is indebted to the Ministry of Education, Science, Sports and Culture of Japan for a scholarship (2000–2004). Another author (L. M. G.) acknowledges the support he has received from the Ministry through the foreign-researcher (COE) invitation program in 2001. This work was partially funded by a 1996 COE special equipment program from the Ministry.

Presented at the IUVSTA 15th International Vacuum Congress and the AVS International Symposium and the 11th International Conference on Solid Surfaces, San Francisco, CA, 28 October–2 November 2001.

[1]M. Ehsasi, M. Matloch, D. Frank, J. H. Block, K. Christmann, F. S. Rys, and W. Hirschwald, J. Chem. Phys. **91**, 4949 (1989).
[2]M. Eiswirth and G. Ertl, Surf. Sci. **177**, 90 (1986).
[3]M. G. Moula, A. B. P. Mishra, I. Rzeznicka, M. U. Kislyuk, S. Liu, Y. Ohno, and T. Matsushima, Chem. Phys. Lett. **341**, 225 (2001).
[4]T. Matsushima, Heterog. Chem. Rev. **2**, 51 (1995).
[5]G. Ertl, Adv. Catal. **37**, 213 (1990).
[6]S. Nettesheim, A. von Oertzen, H. H. Rotermund, and G. Ertl, J. Chem. Phys. **98**, 9977 (1993).
[7]A. von Oertzen, A. S. Mikhailov, H. H. Rotermund, and G. Ertl, J. Phys. Chem. B **102**, 4966 (1998).
[8]J. Wintterlin, Adv. Catal. **45**, 131 (2000).
[9]J. E. Reutt-Robey, D. J. Doren, Y. J. Chabal, and S. B. Christman, Phys. Rev. Lett. **61**, 2778 (1998).
[10]C. T. Campbell, G. Ertl, H. Kuipers, and J. Segner, J. Chem. Phys. **73**, 5862 (1980).
[11]G. Cao, Y. Seimiya, and T. Matsushima, J. Mol. Catal. **141**, 63 (1999).
[12]G. Comsa, R. David, and B. J. Schumacher, Rev. Sci. Instrum. **52**, 789 (1981).
[13]Y. Ohno, T. Matsushima, and H. Uetsuka, J. Chem. Phys. **101**, 5319 (1994).
[14]G. Comsa and R. David, Surf. Sci. Rep. **5**, 1 (1985).
[15]M. W. Roberts and C. S. McKee, in Chemistry of the Metal-Gas Interface (Oxford University Press, New York, 1978), p. 160.
[16]T. Matsushima, J. Chem. Phys. **91**, 5722 (1989).
[17]T. Matsushima, Y. Ohno, and K. Nagai, J. Chem. Phys. **94**, 704 (1991).
[18]G. Cao, M. G. Moula, Y. Ohno, and T. Matsushima, J. Phys. Chem. B **103**, 3235 (1999).
[19]J. Fair, R. J. Madix, J. Chem. Phys. **73**, 3480 (1980).